ORIGINAL PAPER

Effects of niobium doping on lead zirconate titanate films deposited by a sol–gel route

K. W. Kwok · R. C. W. Tsang · H. L. W. Chan · C. L. Choy

Abstract Niobium (Nb)-doped lead zirconate titanate (PZT) films have been prepared on platinized silicon substrates using a sol–gel method. The Zr/Ti ratios of the films are 53/47 and 40/60, and the Nb doping level ranges from 0 mol% to 3 mol%. Similar to the cases in bulk ceramics, after the doping with Nb, the remanent polarization P_r, effective transverse piezoelectric coefficients $e_{31,c}$ and pyroelectric coefficient p of the PZT films increase; but the longitudinal effective piezoelectric coefficient $d_{33,c}$ remains roughly unchanged. At the optimum Nb doping levels, the observed P_r, $-e_{31,c}$ and p reach a maximum value of 30 μC/cm^2, 18 C/m^2 and 350 μC/m^2 K, respectively, for the PZT (53/47) films, and 37 μC/cm^2, 7.9 c/m^2 and 370 μC/m^2 K for the PZT (40/60) films. Our results also reveal that there exist linear relations between p, $e_{31,c}/\varepsilon_r$ and P_r.

1 Introduction

Lead zirconate titanate (PZT) films have been extensively studied for a variety of applications ranging from non-volatile memories to micro-electro-mechanical systems (MEMS) and electro-optical modulators. It is experimentally known that the piezoelectric and pyroelectric properties of a PZT bulk ceramic are primarily governed by its composition. In general, PZT compositions near the morphotropic phase boundary (i.e. Zr/Ti ∼ 53/47) have large piezoelectric coefficients and electromechanical coupling factors while the compositions close to either the zirconate titanate end or the lead titanate end of the phase diagram possess better pyroelectric properties [1, 2]. Besides the compositions, it is also experimentally known that the piezoelectric and pyroelectric properties of bulk ceramics can be optimized by the addition of dopants [1, 3–6]. For example, by the doping of about 2 mol% niobium (Nb), the longitudinal and transverse piezoelectric coefficients (d_{33} and $-d_{31}$) of a PZT (52/48) ceramic are increased by about 60% and 80%, respectively [1]. On the other hand, by a doping of about 2 mol% europium, the pyroelectric coefficient of a PZT (55/45) ceramic is enhanced by about 160% [6]. The effects of dopants on the dielectric and ferroelectric properties of PZT films have been discussed in a number of recent papers [7, 8]. However, their effects on the piezoelectric and pyroelectric properties of PZT films have not been extensively and systematically studied, and, in particular, have not been correlated with the experimentally-known effects on the corresponding bulk ceramics. Haccart et al. [9, 10] and Remiens et al. [11] have studied the piezoelectric coefficients of Nb-doped PZT films prepared by magnetron sputtering. They reported that the optimum doping level of Nb is about 2 at.%, as in the case for the bulk ceramics. For the Nb-doped film, the observed d_{33} value is about 50% higher as compared to the un-doped PZT film (75 pm/V vs. 50 pm/V), while the observed value of e_{31} remains almost unchanged at a value of about –4 C/m^2.

We have studied the effects of Nb-doping on the piezoelectric and pyroelectric properties of sol–gel-derived PZT films (with a Zr/Ti ratio of 53/47) [12]. Our previous

K. W. Kwok (✉) · R. C. W. Tsang · H. L. W. Chan · C. L. Choy
Department of Applied Physics and Materials Research Centre,
The Hong Kong Polytechnic University, Kowloon,
Hong Kong, China
e-mail: apkwkwok@polyu.edu.hk

results revealed that both the piezoelectric and pyroelectric properties of the films could be improved by the doping. However, as the films were deposited on a rigid silicon substrate, they were tightly clamped by the substrate and hence could not deform freely during the measurements. As a result, the exact improvement in the longitudinal piezoelectric properties could not be evaluated. In the present work, we will extend our studies on the sol–gel-derived PZT films with other composition. The resulting effects of the Nb-doping as well as the substrate clamping on the observed piezoelectric and pyroelectric properties of the films will be investigated.

2 Experimental

Nb-doped PZT films with a Zr/Ti ratio of 53/47 and 40/60, abbreviated as PNZT-5347-x and PNZT-4060-x, respectively, were prepared using a sol–gel method. x is the Nb doping level and was varied from 0 mol% to 3 mol% in this work. A PNZT precursor solution was spin coated on a Pt/Ti/SiO$_2$/Si substrate to give a film of thickness about 100 nm, which was then pyrolyzed at 450 °C for 10 min. After the deposition of three layers, the film was annealed in an oxygen atmosphere at 600 °C for 3 min in a rapid thermal processor. By repeating the process a few times, a PZT film of thickness 1 μm was obtained. The film was then annealed at 680 °C for 20 min in a furnace. A platinum top electrode of diameter 1 mm and thickness 150 nm was deposited on the films by dc sputtering in a pure argon atmosphere.

The crystalline structure of the PZT films was studied using X-ray diffraction (XRD) analysis with nickel-filtered CuK$_\alpha$ radiation (X′pert System, Philips Electronic Instruments), and the microstructure was examined using a scanning electron microscope (SEM, Leica Stereoscan 440). The relative permittivity ε and dielectric loss tan δ at 1 kHz were measured using an impedance analyzer (HP 4194A). A Sawyer-Tower circuit was used to measure the polarization hysteresis (P-E) loop, from which the remanent polarization P$_r$ was determined.

Effective longitudinal and transverse piezoelectric coefficients (d$_{33,c}$ and e$_{31,c}$) were measured using a single beam laser interferometry method and a cantilever deflection technique, respectively. The experimental details of the measurements have been reported in a previous publication [13]. To measure d$_{33,c}$, a small ac field (E) at 15 kHz was applied to the film sample in the thickness direction; and the surface displacement (Δt) induced in the sample was measured using a heterodyne single beam laser interferometer (SH-120, B.M. Industries). d$_{33,c}$ was then calculated as:

$$d_{33,c} = \frac{\Delta t / t}{E} \tag{1}$$

where t is the thickness of the film sample. The substrate bending, which usually induces enormous error in the measurement using the single beam laser interferometry method, was effectively suppressed by gluing the substrate tightly to a large and rigid platform [13]. For the e$_{31,c}$ measurement, a rectangular sample (film/substrate) was bent dynamically at a frequency (f) of 10 Hz; and the current (I$_o$) induced on the film surface was measured using a lock-in amplifier. e$_{31,c}$ was then given by:

$$e_{31,c} = \frac{\ell^3 I_o}{3\pi f A h (1-v) Z_o} \left[\ell - \frac{x_o + x_1}{2} \right]^{-1} \tag{2}$$

where Z$_o$ is the deflection at the free end, A is the area of the top electrode, h is the thickness of the substrate, v is Poisson ratio of the substrate, l is the distance from the clamping edge to the free end of the sample, x$_o$ and x$_1$ are the positions of the electrode extremities in the length direction. In the present work, a v value of 0.172 for the substrate was used in the calculation [14].

The pyroelectric coefficient p was measured using a dynamic method. Experimental details of the measurement have been reported in a previous publication [15]. The sample temperature was sinusoidally modulated at room temperature at a frequency (f) of 5 mHz and an amplitude (T$_o$) of 1 K using a Peltier element.; and the 90° out of phase component of the resulting pyroelectric current (I$_p$) with respect to the temperature modulation was measured using a lock-in amplifier. p was then given by:

$$p = \frac{I_p}{2\pi f A T_o} \tag{3}$$

where A is the area of the top electrode. Prior to the measurements of d$_{33,c}$, e$_{31,c}$ and p, the films were poled under a dc field of 20 MV/m at room temperature for 5 min, and then short-circuited for 10 min to remove the conducting charge injected during the poling process.

3 Results and discussion

The XRD patterns of the PNZT-5347-x and PNZT-4060-x films are shown in Figs. 1 and 2, respectively. All the films exhibit a well-crystallized phase with diffraction peaks attributable to the PZT perovskite structure. No pyrochlore or PBO$_x$ phases are observed. There are no significant differences between the diffraction patterns of the films with different Nb doping levels, and most of them exhibit (111)-preferred orientation. As the ionic radius of Nb^{5+} (0.78 Å) is close to and between those of Zr^{4+} and Ti^{4+} (0.86 Å and 0.745 Å, respectively), it is suggested that
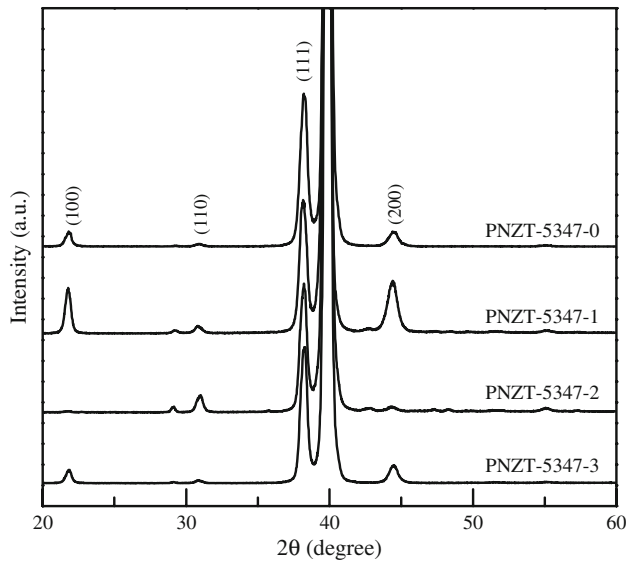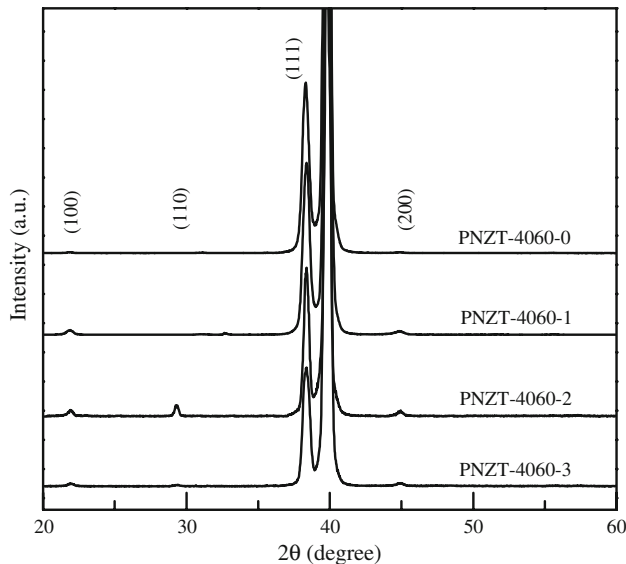
Fig. 1 XRD patterns of the PNZT-5347-x films

Fig. 2 XRD patterns of the PNZT-4060-x films

Fig. 3 SEM micrograph of the cross section of (**a**) the PNZT-5347-2 and (**b**) the PNZT-4060-1 films

Table 1 Relative permittivity ε_r, remanent polarization P_r, effective longitudinal and transverse piezoelectric coefficients $d_{33,c}$ and $e_{31,c}$, and pyroelectric coefficient p of the PNZT-5347-0 and PNZT-4060-0 films

	ε_r	P_r ($\mu C/cm^2$)	$d_{33,c}$ (pm/V)	$e_{31,c}$ (C/m^2)	p ($\mu C/m^2$ K)
PNZT-53/47-0	1100	22.1	97.8	9.3	197
PNZT-40/60-0	830	25.4	35.2	6.3	271

Nb^{5+} may enter the B sites (for Zr^{4+} or Ti^{4+} ions), forming a homogeneous solid solution of similar structures. It has been shown that the solubility limit of Nb^{5+} ions in the perovskite structure could reach close to 7 mol% [16]. Figure 3 shows typical examples of SEM micrograph of the cross section of the PNZT-5347-2 and PNZT-4060-1 films. The films are dense and have columnar grain structure.

The observed ε_r, P_r, $d_{33,c}$, $e_{31,c}$ and p of the PNZT-5347-0 and PNZT-4060-0 (undoped PZT) films are compared in Table 1. Similar to the cases in bulk ceramics, the PNZT-5347-0 film has a higher ε_r than PNZT-406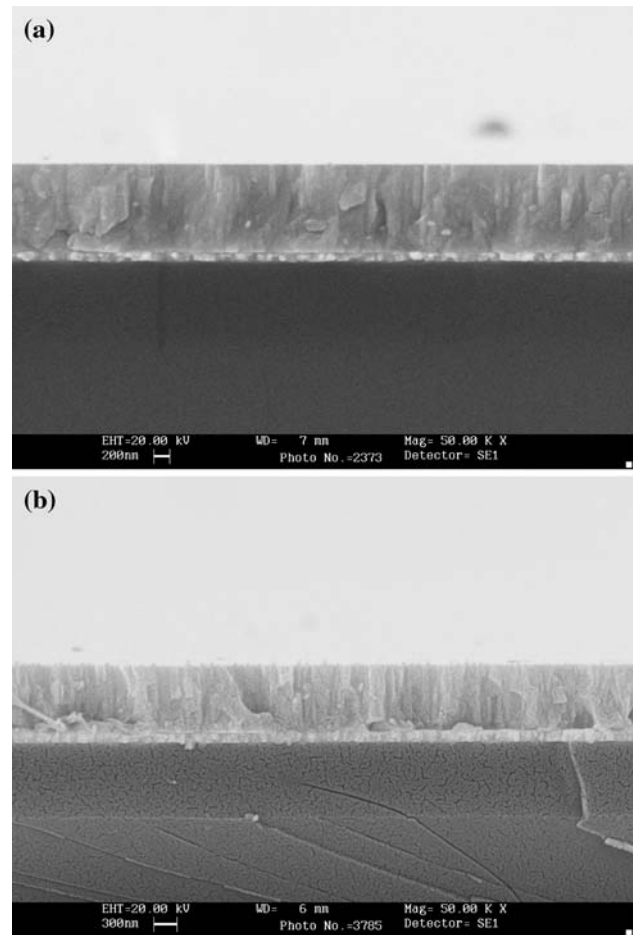0-0 [17]. However, unlike the bulk ceramics where P_r exhibits a maximum at the morphotropic phase boundary [1], the observed P_r of the PNZT-5347-0 film is lower than that of PNZT-4060-0. This difference may arise from that the P_r value obtained in PZT ceramics depends primarily on the ease with which the sample can be poled and not on the intrinsic single crystal value of P_r [18]. Although the PNZT-5347-0 film has a lower P_r, its $d_{33,c}$ and $e_{31,c}$ are higher than those of PNZT-4060-0. This should partly attribute to its larger ε_r value. According to the phenomenological theory, the piezoelectric coefficient d is related to ε_r by [19]:

$$d = 2\varepsilon_r Q P_s \qquad (4)$$

where Q is the electrostrictive coefficient and P_s is the spontaneous polarization. It should also be noted that the observed $d_{33,c}$ and $e_{31,c}$ of the films are not the "true" piezoelectric coefficients. They are the "effective" piezoelectric coefficients owing to the fact that the films are tightly clamped by the substrates and cannot deform freely during the measurements. The clamping effects on the observed piezoelectric coefficients will be further discussed in the following section.

The variations of ε_r with x (Nb doping level) for the Nb-doped PZT films are shown in Fig. 4. As Nb^{5+} has a higher valence than Zr^{4+} and Ti^{4+}, the doping of Nb^{5+} (considered as a donor dopant) creates cation vacancies. Because of the vacancies, the transfer of ions in the lattice is easier than that in a perfect lattice, thus making the movement of domains become easier and the ceramic become "soft". Accordingly, similar to the "softened" bulk ceramics, the observed ε_r of the PNZT-5347-x films increases almost linearly with increasing x. However, it is interesting to note that there is only minimal effect on the PNZT-4060-x films, giving that the observed ε_r remains almost unchanged after the doping of Nb. Unlike ε_r, the observed P_r of both the PNZT-5347-x and PNZT-4060-x films are enhanced, showing an optimum doping level of 2 mol% and 1 mol%, respectively (Fig. 5). Nevertheless, as seen from Fig. 5, the most exact optimum doping level of Nb for the PZT films should be around 1 to 2 mol%. The increase in P_r should be due to the "softening" effect given by Nb^{5+}, as in the cases for bulk ceramics. It is noted that the increments in P_r (in percentage) for both the PNZT-5347-x and PNZT-4060-x films are almost the same, suggesting that the "softening" effect on PZT of different structures are similar.
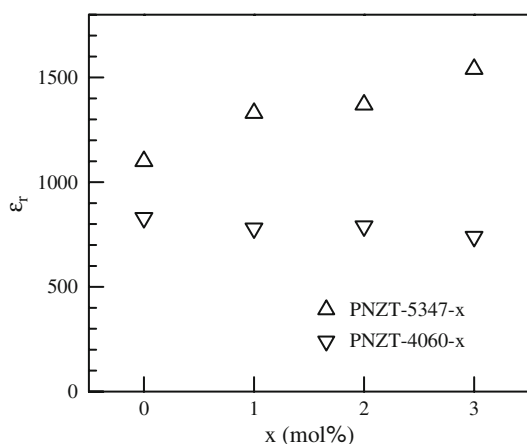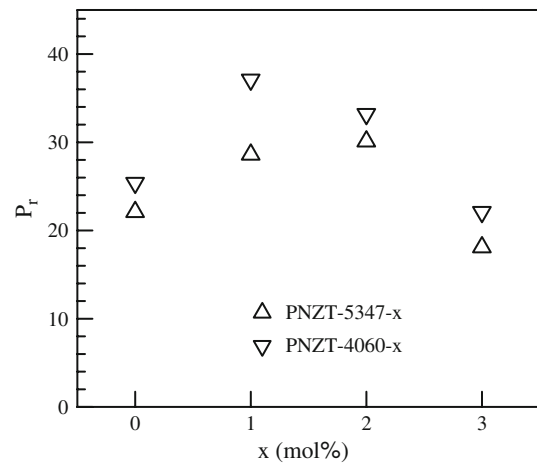

Fig. 5 Variations of the remanent polarization P_r with Nb doping level x

The piezoelectric properties of the Nb-doped PZT films are shown in Figs. 6 and 7. It is seen that, for both the Nb-doped PZT films, the observed $d_{33,c}$ remains roughly unchanged at x < 2 and then decreases with increasing x (Fig. 6). On the other hand, similar to P_r, the observed $-e_{31,c}$ are increased by the doping of Nb and reaches a maximum value at x = 2 mol% and 1 mol% for the PNZT-5347-x and PNZT-4060-x films, respectively (Fig. 7). At the corresponding optimum doping levels, the observed $-e_{31,c}$ is 18 C/m^2 and 7.9 C/m^2, respectively. On the basis of the above results, it seems that the Nb dopant does not afford any improvement in the longitudinal piezoelectric properties of PZT films, which is quite different from the experimentally known effects on bulk ceramics. For a PZT (52/48) bulk ceramic, both the longitudinal and transverse piezoelectric coefficients are increased by a large amount (60% and 80%, respectively) after the doping of 2 mol% Nb [1].
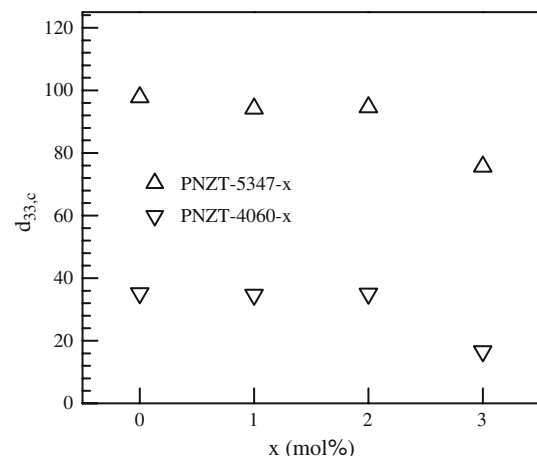

Fig. 4 Variations of the relativity permittivity ε_r with Nb doping level x

Fig. 6 Variations of the effective longitudinal piezoelectric coefficients $d_{33,c}$ with Nb doping level x

Our previous work [12] has shown that this apparent discrepancy can arise from the clamping of the PZT films by the substrate. Because of the clamping, the films cannot deform freely during the measurements, and hence the observed $d_{33,c}$ and $e_{31,c}$ are the effective piezoelectric coefficients, and depend not only on the (true) piezoelectric coefficients (d_{33} and d_{31}) but also on the elastic compliance (s_{11}^E, s_{12}^E and s_{13}^E) of the films [20, 21]:

$$d_{33,c} = d_{33} - \frac{2s_{13}^E d_{31}}{s_{11}^E + s_{12}^E} \qquad (5)$$

$$e_{31,c} = \frac{d_{31}}{s_{11}^E + s_{12}^E} \qquad (6)$$

It is experimentally known that the donor-type dopant (e.g. Nb) can increase not only the piezoelectric properties, but also the elastic compliances of PZT bulk ceramics, and the increments in different material parameters are different. Using the experimentally known material parameters of a PZT (52/48) bulk ceramic [1] and Eqs. 5 and 6, a calculation has shown that, after the doping of 2 mol% Nb, the increment in $d_{33,c}$ is greatly suppressed to 25% as compared to that in d_{33} (60%), while the change in $e_{31,c}$ remains large (67%) as compared that in d_{31} (80%). This is in agreement with our experimental results that there is only a large increase in $e_{31,c}$, but almost no change in $d_{33,c}$ (Figs. 5 and 6).

The variations of the pyroelectric coefficient p with x for the Nb-doped PZT films are shown in Fig. 8. Similar to P_r and $e_{31,c}$, the observed p first increases and then decreases with increasing x, and reaching a maximum value at $x = 2$ mol% and 1 mol% for the PNZT-5347-x and PNZT-4060-x films, respectively. At the corresponding optimum doping levels, the observed p is 350 μC/m^2 K and 370 μC/m^2 K, respectively. This clearly shows that Nb can act to enhance the pyroelectric properties of the PZT films.

Fig. 8 Variation of the pyroelectric coefficient p with Nb doping level x

Although p is defined as the change of the net polarization with increasing temperature, it is still strongly related to the magnitude of the net polarization of a PZT film. Kohli and Muralt have shown that p is linearly proportional to the net polarization of a PZT film [22]. Our experimental results also reveal a similar relation between p and the net polarization, i.e. P_r in this work (Fig. 9). Clearly, according to Eqs. 4–6, there does not exist a simple relation between $d_{31,c}$, $e_{31,c}$ and P_r. However, it is interesting to note a simple relation is obtained between $e_{31,c}/\varepsilon_r$ and P_r (Fig. 10), but not for $d_{33,c}/\varepsilon_r$ and P_r. This should be due to the weaker dependence of $e_{31,c}$ on the elastic compliance as compared to $d_{33,c}$, referring to Eqs. 5 and 6. So, it is suggested that the transverse piezoelectric coefficient $e_{31,c}$ should be used as a measure for evaluating the piezoelectric properties of PZT films.
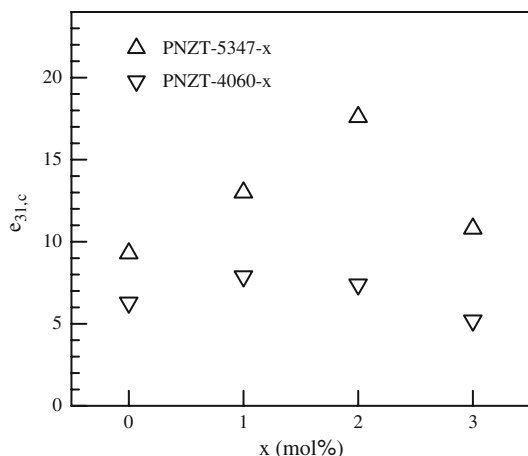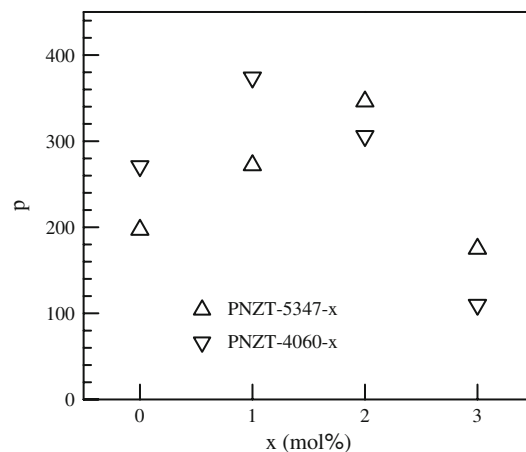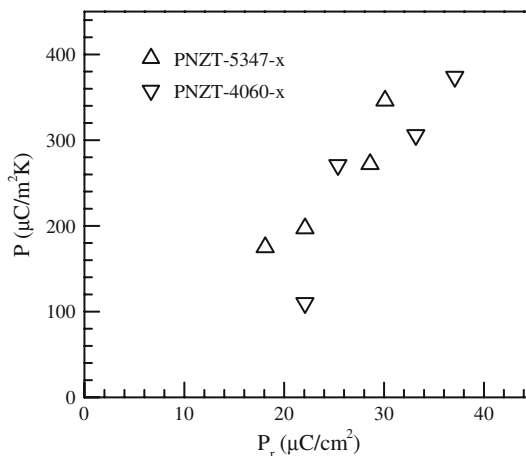

Fig. 7 Variations of the effective transverse piezoelectric coefficients $e_{31,c}$ with Nb doping level x

Fig. 9 Variation of the pyroelectric coefficient p with P_r
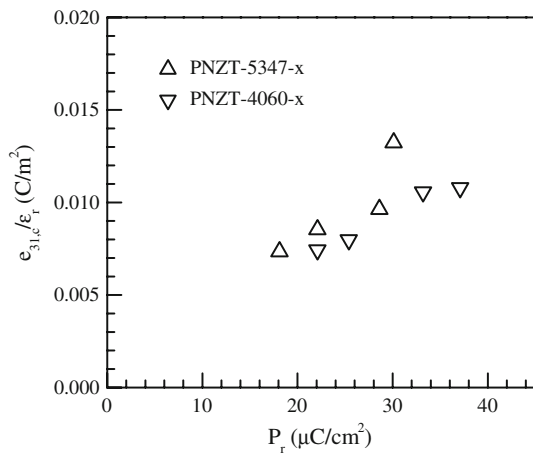
Fig. 10 Variation of $e_{31,c}/\varepsilon_r$ with P_r

4 Conclusion

The Nb effects on the dielectric, ferroelectric, piezoelectric and pyroelectric properties of sol–gel derived PZT films have been studied. Similar to the cases in bulk ceramics, after the doping with Nb, the remanent polarization P_r, effective transverse piezoelectric coefficients $e_{31,c}$ and pyroelectric coefficient p of the PZT films increase; but the longitudinal effective piezoelectric coefficient $d_{33,c}$ remains roughly unchanged. It is suggested that the discrepancy in the observed $d_{33,c}$ arises from the clamping of the films by the substrate. The optimum Nb doping level for improving the piezoelectric and pyroelectric properties of the PNZT-5347-x and PNZT-4060-x films are about 2 mol% and 1 mol%, respectively. For the PNZT-5347-2 film, the observed P_r, $d_{33,c}$, $-e_{31,c}$ and p are 30 μC/cm^2, 95 pm/V, 18 C/m^2 and 350 μC/m^2 K, respectively, while they are 37 μC/cm^2, 35 pm/V, 7.9 C/m^2 and 370 μC/m^2 K, respectively, for the PNZT-4060-1 film. Moreover, linear relation is observed not only between p and P_r, but also between $e_{31,c}/\varepsilon_r$ and Pr.

References

1. Jaffe B, Cook WR Jr, Jaffe H (1971) Piezoelectric ceramics. Academic, New York
2. Whatmore RW, Watton R (2000) Ferroelectrics 236:259
3. Kulcsar F (1959) J Amer Ceram Soc 42:343
4. Takahashi S (1982) Ferroelectrics 41:413
5. Kobune M, Mineshige A, Fujii S, Maeda Y (1997) Jpn J Appl Phys 36:5976
6. Khazanchi R, Sharma S, Goel TC (2005) J Electroceramics 14:113
7. Aggarwal S, Jenkins IG, Nagaraj B, Kerr CJ, Canedy C, Ramesh R, Velasquez G, Boyer L, Evans JT (1999) Appl Phys Lett 75:1787
8. Yang B, Aggarwal S, Dhote AM, Song TK, Ramesh R, Lee JS (1997) Appl Phys Lett 71:356
9. Haccart T, Cattan E, Remiens D (2000) Appl Phys Lett 76:3292
10. Haccart T, Remiens D, Cattan E (2003) Thin Solid Films 423:235
11. Remiens D, Cattan E, Soyer C, Haccart T (2003) Mat Sci Semicon Proc 5:123
12. Kwok KW, Tsang RCW, Chan HLW, Choy CL (2004) J Appl Phys 95:1372
13. Tsang RCW, Kwok KW, Chan HLW, Choy CL (2002) Integr Ferroelectrics 50:143
14. Shepard JF, Chu F, Kanno I, Trolier-McKinstry S (1998) Sensor Actuat A 71:133
15. Dias C, Simon M, Quad R, Das-Gupta DK (1993) J Phys D 26:106
16. Pereira M, Peixoto AG, Gomes MJM (2001) J Eur Ceram Soc 21:1353
17. Jaffe B, Roth RS, Marzullo S (1954) J Appl Phys 25:809
18. Auciello O, Foster CM, Ramesh R (1998) Annu Rev Mater Sci 28:501
19. Damjanovic D (1998) Rep Prog Phys 61:1267
20. Kholkin A, Wutchrich C, Taylor DV, Setter N (1996) Rev Sci Instr 67:1935
21. Dubois MA, Muralt P (1999) Sensor Actuat A 77:106
22. Kohli M, Muralt P (1999) Ferroelectrics 225:155